Sorbonne Université
Master 1 Mathématiques et applications

4MA106 Fondements des méthodes numériques

Projet TP 1

Approximation de l'équation de transport à vitesse constante

Nom :	Thomas Gantz
Numéro de étudiant :	21109004
Enseignant :	Ruiyang Dai
Date de remise :	30.12.2024

Abstract

The goal of this TP is to numerically solve the transport equation with constant speed, i.e., find:

$$\bar{u} : \mathbb{R} \times (0, T) \to \mathbb{R},$$

the solution of the following problem:

$$\begin{cases} \partial_t \bar{u}(x,t) + a\, \partial_x \bar{u}(x,t) = 0, & \forall (x,t) \in \mathbb{R} \times (0,T),\ T > 0, \\ \bar{u}(x,0) = u_{\mathrm{ini}}(x), & \forall x \in \mathbb{R}. \end{cases} \tag{P}$$

In particular, we restrict ourselves to a 1-periodic initial condition u_{ini}.

Contents

1 Mathematical Foundations

1.1 Periodicity

By the method of characteristics, one can determine the analytical solution:

$$\bar{u}(x,t) = u_{\text{ini}}(x - at), \quad \forall (x,t) \in \mathbb{R} \times (0,T).$$

In particular, this solution is also 1-periodic (Exo 1), and the restriction to a finite domain therefore still determines the entire solution.

Proof. To show that the solution is 1-periodic, we need to verify the following property:

$$\bar{u}(x+1,t) = \bar{u}(x,t), \quad \forall (x,t) \in \mathbb{R} \times (0,T).$$

Using the expression for $\bar{u}(x,t)$, we compute:

$$\bar{u}(x+1,t) = u_{\text{ini}}((x+1) - at) = u_{\text{ini}}(x - at + 1).$$

Since the initial condition $u_{\text{ini}}(x)$ is 1-periodic, we have:

$$u_{\text{ini}}(x - at + 1) = u_{\text{ini}}(x - at).$$

Therefore:

$$\bar{u}(x+1,t) = \bar{u}(x,t), \quad \forall (x,t) \in \mathbb{R} \times (0,T).$$

□

Consider the initial condition $u_{\text{ini}}(x) = \sin(2\pi x)$, $\forall x \in \mathbb{R}$, which is 1-periodic (Exo 2).

Proof. By the 2π-periodicity of the sine function, we compute:

$$u_{\text{ini}}(x+1) = \sin(2\pi(x+1)) = \sin(2\pi x + 2\pi) = \sin(2\pi x) = u_{\text{ini}}(x), \quad \forall x \in \mathbb{R}.$$

□

1.2 Schemes

We are analyzing the following 3-point schemes (Exo 3.3):

Scheme	$\mathbf{c_{-1}}$	$\mathbf{c_0}$	$\mathbf{c_1}$
Centré	$\frac{\lambda a}{2}$	1	$-\frac{\lambda a}{2}$
Décentré à gauche	λa	$1-\lambda a$	0
Décentré à droite	0	$1+\lambda a$	$-\lambda a$
Lax-Friedrichs	$\frac{1+\lambda a}{2}$	0	$\frac{1-\lambda a}{2}$
Lax-Wendroff	$\frac{\lambda^2 a^2+\lambda a}{2}$	$1-\lambda^2 a^2$	$\frac{\lambda^2 a^2-\lambda a}{2}$

Table 1.1: Coefficients c_{-1}, c_0, and c_1 of the 3-point schemes

Taking into account the periodicity, this leads to the iteration matrix:

$$Q = \begin{bmatrix} c_0 & c_1 & 0 & \cdots & 0 & c_{-1} \\ c_{-1} & c_0 & c_1 & \cdots & 0 & 0 \\ 0 & c_{-1} & c_0 & \cdots & 0 & 0 \\ \vdots & \vdots & \vdots & \ddots & \vdots & \vdots \\ 0 & 0 & 0 & \cdots & c_0 & c_1 \\ c_1 & 0 & 0 & \cdots & c_{-1} & c_0 \end{bmatrix} \in \mathbb{R}^{J \times J}$$

1.3 Convergence

Now, we aim to analyze the convergence of the proposed schemes. According to the Lax theorem, convergence is equivalent to consistency and stability.

The analysis shall be performed in an appropriate norm. It is crucial to note that iteration vectors grow with finer discretizations in space. This growth does not affect the infinity norm, and hence the discrete infinity norm coincides with the standard infinity norm.

However, the discrete 2-norm is sensitive to the scaling of the vector length and would diverge unless appropriately scaled. To address this, the discrete 2-norm is scaled by the grid spacing Δx, such that:

$$\|v\|_{2,\Delta} = \sqrt{\Delta x} \cdot \left(\sum_i^n |v_i|^2 \right)^{1/2}.$$

In this scaled norm, the convergence properties can be rigorously analyzed. The scaling ensures that the norm remains bounded as the grid is refined, enabling the comparison of numerical solutions across different discretizations.

1.3.1 Consistency

We start by analyzing the consistency. Therefore, we investigate κ_n^j, the consistency error of the method described at the spatial point x_j and time t_n. From this, we can estimate the consistency errors of the aforementioned schemes in the $\|\cdot\|_\infty$-norm. Consequently, this also provides an estimate for the $\|\cdot\|_{2,\Delta}$-norm, as the latter is bounded above by the former:

$$\|v\|_{2,\Delta} \leq \sqrt{n\Delta x}\, \|v\|_\infty,$$

where $n\Delta x = 1$ corresponds to the discretization of the spatial domain.

We further assume sufficient smoothness of the solution, ensuring that its derivatives are continuous and bounded on compact sets. This assumption is satisfied in our case, as the solution $\sin(x - at)$ is C^∞ (infinitely differentiable).

Centré: $\kappa_n^j = O(\Delta t) + O((\Delta x)^2)$.

Proof. We start with the definition:

$$\kappa_n^j = \frac{1}{\Delta t}\left(u(x_j, t_{n+1}) - u(x_j, t_n)\right) + \frac{a}{2\Delta x}\left(u(x_{j+1}, t_n) - u(x_{j-1}, t_n)\right)$$

which can be approximated by a Taylor-Lagrange expansion. First, we expand $u(x_j, t_{n+1})$, $u(x_{j+1}, t_n)$, and $u(x_{j-1}, t_n)$ in Taylor series about t_n and x_j:

$$u(x_j, t_{n+1}) = u(x_j, t_n) + \Delta t \frac{\partial u}{\partial t}(x_j, t_n) + O(\Delta t^2),$$

$$u(x_{j+1}, t_n) = u(x_j, t_n) + \Delta x \frac{\partial u}{\partial x}(x_j, t_n) + O((\Delta x)^2),$$
$$u(x_{j-1}, t_n) = u(x_j, t_n) - \Delta x \frac{\partial u}{\partial x}(x_j, t_n) + O((\Delta x)^2).$$

Substituting these expansions into the formula for κ_n^j:

$$\kappa_n^j = \frac{1}{\Delta t}\left(u(x_j, t_n) + \Delta t \frac{\partial u}{\partial t}(x_j, t_n) + O(\Delta t^2) - u(x_j, t_n)\right)$$

$$+\frac{a}{2\Delta x}\left(u(x_j,t_n)+\Delta x\frac{\partial u}{\partial x}(x_j,t_n)+O((\Delta x)^2)-u(x_j,t_n)+\Delta x\frac{\partial u}{\partial x}(x_j,t_n)+O((\Delta x)^2)\right)$$
$$=(\partial_t u(x_j,t_n)+O(\Delta t))+a\left(\partial_x u(x_j,t_n)+O((\Delta x)^2)\right).$$

Since u is a solution to the PDE, the consistency error is $O(\Delta t)+O((\Delta x)^2)$. □

Décentré à gauche: $\kappa_n^j=O(\Delta t)+O(\Delta x)$.

Proof.

$$\kappa_n^j=\frac{1}{\Delta t}\left(u(x_j,t_{n+1})-u(x_j,t_n)\right)+\frac{a}{\Delta x}\left(u(x_j,t_n)-u(x_{j-1},t_n)\right)$$
$$=(\partial_t u(x_j,t_n)+O(\Delta t))+a\left(\partial_x u(x_j,t_n)+O(\Delta x)\right).$$

□

Décentré à droite: $\kappa_n^j=O(\Delta t)+O(\Delta x)$.

Proof.

$$\kappa_n^j=\frac{1}{\Delta t}\left(u(x_j,t_{n+1})-u(x_j,t_n)\right)+\frac{a}{\Delta x}\left(u(x_{j+1},t_n)-u(x_j,t_n)\right)$$
$$=(\partial_t u(x_j,t_n)+O(\Delta t))+a\left(\partial_x u(x_j,t_n)+O(\Delta x)\right).$$

□

Lax-Friedrichs: $\kappa_n^j=O(\Delta t)+O((\Delta x)^2/\Delta t)$.

Proof. For the Lax-Friedrichs method, we have the following update formula:

$$u_j^{n+1}=\frac{1}{2}\left(u_{j+1}^n+u_{j-1}^n\right)-\frac{\lambda a}{2}\left(u_{j+1}^n-u_{j-1}^n\right),$$

where $\lambda=\frac{\Delta t}{\Delta x}$. Expanding u_{j+1}^n and u_{j-1}^n using Taylor expansions around x_j, we have:

$$u_{j+1}^n=u_j^n+\Delta x\frac{\partial u}{\partial x}(x_j,t_n)+\frac{(\Delta x)^2}{2}\frac{\partial^2 u}{\partial x^2}(x_j,t_n)+O((\Delta x)^3),$$
$$u_{j-1}^n=u_j^n-\Delta x\frac{\partial u}{\partial x}(x_j,t_n)+\frac{(\Delta x)^2}{2}\frac{\partial^2 u}{\partial x^2}(x_j,t_n)+O((\Delta x)^3).$$

Simplifying the expression:

$$u_j^{n+1} = u_j^n + O((\Delta x)^2) - \lambda a \left(\Delta x \frac{\partial u}{\partial x}(x_j, t_n) + O((\Delta x)^3) \right).$$

.

Simplifying further:

$$u_j^{n+1} = u_j^n + O((\Delta x)^2) - \Delta t (a \frac{\partial u}{\partial x}(x_j, t_n) + O((\Delta x)^2)).$$

Thus, the consistency error is:

$$O(\Delta t) + O((\Delta x)^2 / \Delta t).$$

Therefore, the Lax-Friedrichs method is consistent of order 1 in time and order 1 in space under the condition that $\frac{(\Delta x)^2}{\Delta t}$ tends to 0. In other words, the condition requires that Δx tends to 0 faster than $\sqrt{\Delta t}$. □

Lax-Wendroff: $\kappa_n^j = O((\Delta t)^2) + O((\Delta x)^2)$.

Proof. We start with the Lax-Wendroff method, which has the following update formula:

$$u_j^{n+1} = u_j^n - \frac{\lambda a}{2} \left(u_{j+1}^n - u_{j-1}^n \right) + \frac{\lambda^2 a^2}{2} \left(u_{j+1}^n - 2u_j^n + u_{j-1}^n \right),$$

where $\lambda = \frac{\Delta t}{\Delta x}$.

Next, we perform a Taylor expansion of the terms u_{j+1}^n and u_{j-1}^n around x_j at time t_n:

$$u_{j+1}^n = u_j^n + \Delta x \frac{\partial u}{\partial x}(x_j, t_n) + \frac{(\Delta x)^2}{2} \frac{\partial^2 u}{\partial x^2}(x_j, t_n) + O((\Delta x)^3),$$

$$u_{j-1}^n = u_j^n - \Delta x \frac{\partial u}{\partial x}(x_j, t_n) + \frac{(\Delta x)^2}{2} \frac{\partial^2 u}{\partial x^2}(x_j, t_n) + O((\Delta x)^3).$$

Now, substitute these expansions into the update formula for u_j^{n+1} and simplify.

Simplifying the first term:

$$-\frac{\lambda a}{2} \left(u_{j+1}^n - u_{j-1}^n \right) = -\frac{\lambda a}{2} \left(2\Delta x \frac{\partial u}{\partial x}(x_j, t_n) + O((\Delta x)^3) \right)$$

Simplifying the second term:

$$\frac{\lambda^2 a^2}{2}\left(u_{j+1}^n - 2u_j^n + u_{j-1}^n\right) = \frac{\lambda^2 a^2}{2}\left(2\Delta x^2 \frac{\partial^2 u}{\partial x^2}(x_j, t_n) + O((\Delta x)^4)\right)$$

Now, combining the terms, we have:

$$u_j^{n+1} = u_j^n - a\Delta t \frac{\partial u}{\partial x}(x_j, t_n) + a^2 \Delta t^2 \frac{\partial^2 u}{\partial x^2}(x_j, t_n) + O((\Delta x)^2 \Delta t).$$

Expanding u_j^{n+1} in a Taylor series gives:

$$u_j^{n+1} - u_j^n + a\Delta t \frac{\partial u}{\partial x}(x_j, t_n) = \Delta t^2 \frac{\partial^2 u}{\partial t^2}(x_j, t_n) + O((\Delta t)^3).$$

Using the derived transport equation:

$$\frac{\partial^2 u}{\partial t^2}(x_j, t_n) = a^2 \frac{\partial^2 u}{\partial x^2}(x_j, t_n),$$

we find that the consistency error is:

$$O(\Delta t^2) + O(\Delta x^2).$$

Therefore, the Lax-Wendroff method is consistent of order 2 in time and space. □

1.3.2 Stability

Now we analyze the stability (Exo 4) and determine a CFL condition for stability (regarding $\lambda > 0$ and a).

Remark. The discrete norm for matrices is the matrix norm:

$$\|Q\|_\Delta = \sup_{x \neq 0} \frac{\sqrt{\Delta x}\|Qx\|}{\sqrt{\Delta x}\|x\|} = \sup_{x \neq 0} \frac{\|Qx\|}{\|x\|} = \|Q\|.$$

Using the submultiplicativity of matrix norms:

$$\|Q^n\| \leq \|Q\|^n,$$

stability is ensured if $\|Q\| \leq 1$, as $\|Q^n\|$ remains bounded for all $n \in \mathbb{N}$.

Infinity Norm

Centré: No condition.

Proof.

$$\|Q\|_\infty = 1 + \left|\frac{\lambda a}{2}\right| + \left|-\frac{\lambda a}{2}\right| > 1.$$

□

Décentré à gauche: $a > 0, \lambda \leq \frac{1}{|a|}$.

Proof.

$$\|Q\|_\infty = |\lambda a| + |1 - \lambda a| = (\lambda a) + (1 - \lambda a) = 1.$$

□

Décentré à droite: $a < 0, \lambda \leq \frac{1}{|a|}$.

Proof.

$$\|Q\|_\infty = |1 + \lambda a| + |-\lambda a| = (1 + \lambda a) + (-\lambda a) = 1.$$

□

Note: The upwind method adapts to the sign of a, employing a "décentré à gauche" scheme for $a > 0$ and a "décentré à droite" scheme for $a < 0$. This approach ensures numerical stability by aligning the discretization direction with the sign of a.

Lax-Friedrichs: $\lambda \leq \frac{1}{|a|}$.

Proof.

$$\|Q\|_\infty = \left|\frac{1 + \lambda a}{2}\right| + \left|\frac{1 - \lambda a}{2}\right| = \left(\frac{1 + \lambda a}{2}\right) + \left(\frac{1 - \lambda a}{2}\right) = 1.$$

□

Lax-Wendroff: $\lambda = \frac{1}{|a|}$

Note: The scheme then corresponds to Lax-Friedrichs, so no additional benefit in order is gained.

Proof. For the Lax-Wendroff scheme, we compute the infinity norm:

$$\|Q\|_\infty = \left|\frac{\lambda^2 a^2 + \lambda a}{2}\right| + |1 - \lambda^2 a^2| + \left|\frac{\lambda^2 a^2 - \lambda a}{2}\right|.$$

For a similar argumentation, the term $|1 - \lambda^2 a^2|$ must satisfy:

$$\lambda^2 a^2 \leq 1, \quad \text{implying} \quad \lambda \leq \frac{1}{|a|}.$$

For the left-hand term $\left|\frac{\lambda^2 a^2 + \lambda a}{2}\right|$ and $a < 0$, we require:

$$\lambda^2 a^2 \geq \lambda a, \quad \text{implying} \quad \lambda \geq \frac{1}{|a|}.$$

Similarly, for the right-hand term $\left|\frac{\lambda^2 a^2 - \lambda a}{2}\right|$, the same inequality holds for $a > 0$. □

2-Norm

We are using the von Neumann stability criterion, i.e., the scheme is stable in the 2-norm if and only if for all $k = 0, \ldots, M$, where $\theta_k = k\Delta x$:

$$|\alpha_k| = \left|\sum_{l=-1}^{1} c_l \exp(2i\pi l \theta_k)\right| \leq 1.$$

In the following proofs, we use Euler's formula, $e^{ix} = \cos(x) + i\sin(x)$, and the symmetry properties of sine and cosine: $\sin(-x) = -\sin(x)$, $\cos(-x) = \cos(x)$. Let $\theta = 2\pi k\Delta x$ for some k.

Centré: No condition.

Proof. We have

$$\alpha_k = \frac{\lambda a}{2} e^{-i\theta} + 1 - \frac{\lambda a}{2} e^{i\theta}.$$

Simplifying using Euler's formula:

$$\alpha_k = 1 + \frac{\lambda a}{2} \left(e^{-i\theta} - e^{i\theta} \right) = 1 - i\lambda a \sin(\theta).$$

Thus,

$$|\alpha_k| = \sqrt{1 + (\lambda a \sin(\theta))^2}.$$

Since $\sqrt{1 + (\lambda a \sin(\theta))^2} > 1$ for $\theta \neq 0$, the scheme is not stable. □

Décentré à gauche: $a > 0$, $\lambda \leq \frac{1}{|a|}$.

Proof. For the left-biased scheme,

$$\alpha_k = \lambda a e^{-i\theta} + 1 - \lambda a.$$

The term α_k lies on a circle with center $1 - \lambda a$ and radius λa. Thus, the magnitude $|\alpha_k|$ is bounded by:

$$|\alpha_k| \leq \max\left(1, |1 - 2\lambda a|\right).$$

□

Décentré à droite: $a < 0$, $\lambda \leq \frac{1}{|a|}$.

Proof. For the right-biased scheme,

$$\alpha_k = 1 + \lambda a - \lambda a e^{i\theta}.$$

The term α_k lies on a circle with center $1 + \lambda a$ and radius λa. Thus, the magnitude $|\alpha_k|$ is bounded by:

$$|\alpha_k| \leq \max\left(1, |1 + 2\lambda a|\right).$$

□

Lax-Friedrichs: $\lambda \leq \frac{1}{|a|}$.

Proof. For the Lax-Friedrichs method, we have:

$$\alpha_k = \cos(\theta) - i\lambda a \sin(\theta).$$

To determine stability, we compute the magnitude:

$$|\alpha_k|^2 = \cos^2(\theta) + (\lambda a)^2 \sin^2(\theta).$$

Using the Pythagorean identity $\cos^2(\theta) + \sin^2(\theta) = 1$, we obtain:

$$|\alpha_k|^2 = 1 + \big((\lambda a)^2 - 1\big)\sin^2(\theta).$$

For stability, we require $|\alpha_k|^2 \leq 1$. This is satisfied if:

$$\big((\lambda a)^2 - 1\big)\sin^2(\theta) \leq 0.$$

Since $\sin^2(\theta) \geq 0$, this condition holds if and only if:

$$(\lambda a)^2 \leq 1 \quad \Rightarrow \quad \lambda \leq \frac{1}{|a|}.$$

Thus, the Lax-Friedrichs method is stable under the CFL condition $\lambda \leq \frac{1}{|a|}$. □

Lax-Wendroff: $\lambda \leq \frac{1}{|a|}$.

Proof. For the Lax-Wendroff method, we have:

$$\alpha_k = 1 - 2(\lambda a)^2 \sin^2(\theta) - i\lambda a \sin(2\theta).$$

To determine stability, we compute the magnitude:

$$|\alpha_k|^2 = \big(1 - 2(\lambda a)^2 \sin^2(\theta)\big)^2 + (\lambda a \sin(2\theta))^2.$$

Expanding the first term:

$$\big(1 - 2(\lambda a)^2 \sin^2(\theta)\big)^2 = 1 - 4(\lambda a)^2 \sin^2(\theta) + 4(\lambda a)^4 \sin^4(\theta).$$

Using the double-angle identity $\sin(2\theta) = 2\sin(\theta)\cos(\theta)$, the second term becomes:

$$(\lambda a \sin(2\theta))^2 = 4(\lambda a)^2 \sin^2(\theta)\cos^2(\theta).$$

Substituting these expressions, we have:

$$|\alpha_k|^2 = 1 - 4(\lambda a)^2 \sin^2(\theta) + 4(\lambda a)^4 \sin^4(\theta) + 4(\lambda a)^2 \sin^2(\theta)\cos^2(\theta).$$

Simplifying further:

$$|\alpha_k|^2 = 1 + 4(\lambda a)^2 \sin^2(\theta)\left((\lambda a)^2 \sin^2(\theta) + \cos^2(\theta) - 1\right).$$

For stability, we require $|\alpha_k|^2 \leq 1$, which holds if:

$$(\lambda a)^2 \sin^2(\theta) + \cos^2(\theta) \leq 1.$$

This condition holds if $\lambda \leq \frac{1}{|a|}$ (see above). $\square$

The following table summarizes the results regarding the consistency errors and stability conditions:

Finite Difference Schemes	
Consistency Errors	
Centré	$O(\Delta t) + O((\Delta x)^2)$
Décentré à gauche	$O(\Delta t) + O(\Delta x)$
Décentré à droite	$O(\Delta t) + O(\Delta x)$
Lax-Friedrichs	$O(\Delta t) + O\left(\frac{(\Delta x)^2}{\Delta t}\right)$
Lax-Wendroff	$O((\Delta t)^2) + O((\Delta x)^2)$
Stability Conditions	
L^∞ **Norm:**	
Centré	None
Décentré à gauche	$a > 0,\ \lambda \leq \frac{1}{|a|}$
Décentré à droite	$a < 0,\ \lambda \leq \frac{1}{|a|}$
Lax-Friedrichs	$\lambda \leq \frac{1}{|a|}$
Lax-Wendroff	None
L^2 **Norm:**	
Centré	None
Décentré à gauche	$a > 0,\ \lambda \leq \frac{1}{|a|}$
Décentré à droite	$a < 0,\ \lambda \leq \frac{1}{|a|}$
Lax-Friedrichs	$\lambda \leq \frac{1}{|a|}$
Lax-Wendroff	$\lambda \leq \frac{1}{|a|}$

Table 1.2: Consistency and stability

2 Implementation

This chapter presents the numerical implementation. The implementation emphasizes modularity, clarity, and adaptability, ensuring a robust and extensible code base.

2.1 Highlights

The numerical and analytical solutions are compared interactively using `Plotly`, allowing dynamic plots. These are rendered in the browser, when executing the Python script.

The finite difference schemes are defined in a Python dictionary structure. Each scheme is represented by its corresponding coefficients for the three-point stencil. This dictionary-based implementation facilitates extensibility, allowing new schemes to be added or existing ones to be modified without altering the overall structure.

The periodicity is used during each time iteration step. This ensures that the values wrap around correctly at the domain boundaries, preserving the 1-periodicity of the solution.

2.2 Function Breakdown

`espaceDiscretise(J: int, lam: float)` $\rightarrow$ `tuple[float, float, np.ndarray, int]`

Purpose: Handles the spatial and temporal discretization of the problem.
Parameters:

- J: Number of spatial steps (grid points).
- λ: CFL condition parameter, affecting time step size relative to spatial step.

Returns:

- dx: Spatial step size.
- dt: Temporal step size, calculated based on λ and dx.
- X: Array of spatial points $[0, 1)$ with J discretization points.
- M: Number of time steps calculated from the total time T and time step dt.

This function sets up the spatial and temporal grid, calculating step sizes and the number of time steps needed for the solution.

`schema(dx: float, dt: float, X: np.ndarray, M: int, c_1: float, c0: float, c1: float) → tuple[np.ndarray, np.ndarray, float, float]`

Purpose: Computes the numerical solution using a finite difference scheme.

Parameters:

- dx: Spatial step size.
- dt: Temporal step size.
- X: Array of spatial points.
- M: Number of time steps.
- c_{-1}, c_0, c_1: Coefficients for the left, central, and right points in the finite difference scheme.

Returns:

- *Uh*: Numerical solution at the final time step.
- *Ub*: Analytical solution at the final time step for comparison.
- *errL2*: Discrete L2 norm of the error (measure of overall error in the solution).
- *errInf*: Infinity norm of the error (maximum absolute error).

This function computes the numerical solution at each time step using the provided finite difference coefficients. The error between the numerical and analytical solution is calculated using both discrete L2 and infinity norms.

`numerical_solution(Schema: dict, J: int) → None`

Purpose: Plots the analytical and numerical solutions for all defined finite difference schemes.

Parameters:

- *Schema*: Dictionary of finite difference schemes with their corresponding coefficients.
- J: Number of spatial discretization points.

Returns: None (the function generates a plot).

This function computes the numerical solutions using the provided schemes and compares them to the analytical solution at each time step. The comparison is visualized using `Plotly` to render dynamic plots.

`determine_Q(c_1: float, c0: float, c1: float, J: int) → np.ndarray`

Purpose: Constructs the iteration matrix Q for a three-point finite difference scheme.

Parameters:

- c_{-1}, c_0, c_1: Coefficients for the left, central, and right points in the finite difference scheme.
- J: Number of spatial discretization points.

Returns:

- Q: Iteration matrix of size *(J, J)*, used for stability analysis.

This function constructs the iteration matrix Q based on the finite difference coefficients and the number of spatial points. It also ensures periodicity by wrapping around the boundary points.

`plot_norm_Qn(Schema: dict, J: int) -> None`

Purpose: Plots the L2 and infinity norms of the powers of the iteration matrix Q for each scheme over time steps.

Parameters:

- *Schema*: Dictionary of schemes with coefficients.
- J: Number of spatial discretization points.

Returns: None (the function generates a plot).

This function computes the matrix powers Q^n for each time step n and plots the

L2 and infinity norms of these powers for stability analysis. It helps visualize how the norms evolve over time for different schemes, providing insight into their stability.

`convergenceDeltaX(Schema: dict, J: list[int])` $\rightarrow$ `None`

Purpose: Plots the error convergence with respect to the spatial step size dx for different schemes.

Parameters:

- *Schema*: Dictionary of schemes with coefficients.
- J: List of different spatial discretization point counts to assess convergence.

Returns: None (the function generates a plot).

For each spatial resolution J, this function computes the numerical solution and the corresponding errors in the discrete L2 and infinity norms. It then plots these errors as a function of dx, which helps assess how the solution converges with decreasing spatial step size.

3 Evaluation

In the following section, we evaluate the obtained numerical results and check for coherence with the theory. We fix $\lambda = 0.8$ and $a = 1$ (which satisfies the determined CFL condition, see Tabl 1.2), and set $T = 0.75$ and $J = 20$ for the base case, with $J = 25, 50, 100, 200$ used for the convergence analysis.

First, we examine the numerical solutions obtained against the analytical solution (Exo 3.3). Then, we check for stability (Exo 4), as we have identified this as a potential issue. Finally, we investigate the order of convergence (Exo 5).

3.1 Solution

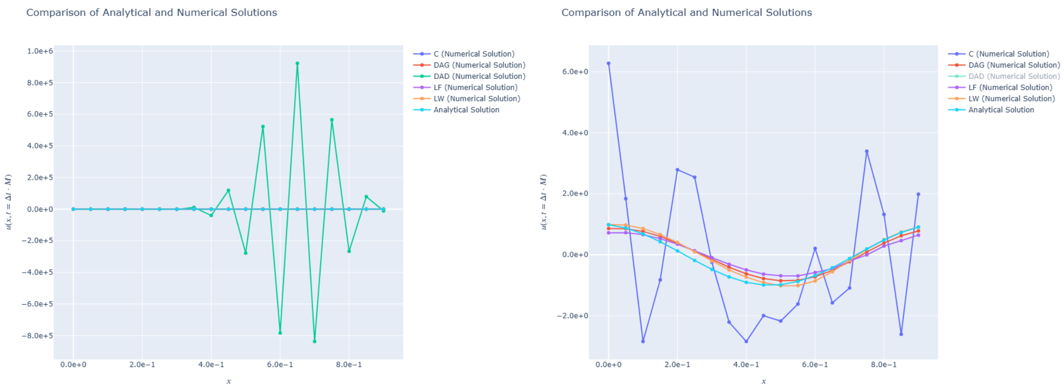

Figure 3.1: Comparison of numerical solutions with the analytical solution

It can be seen that the schemes *décentré à droite* (DAD) and *centré* (C) do not align with the analytical solution, while *décentré à gauche* (DAG), Lax-Friedrichs (LF), and Lax-Wendroff (LW) do.

This matches our expectation since the centered scheme is generally not stable, and the *décentré à droite* scheme is unstable in this case when $a > 0$, while the other schemes satisfy their CFL condition $\lambda \leq \frac{1}{|a|}$.

3.2 Stability

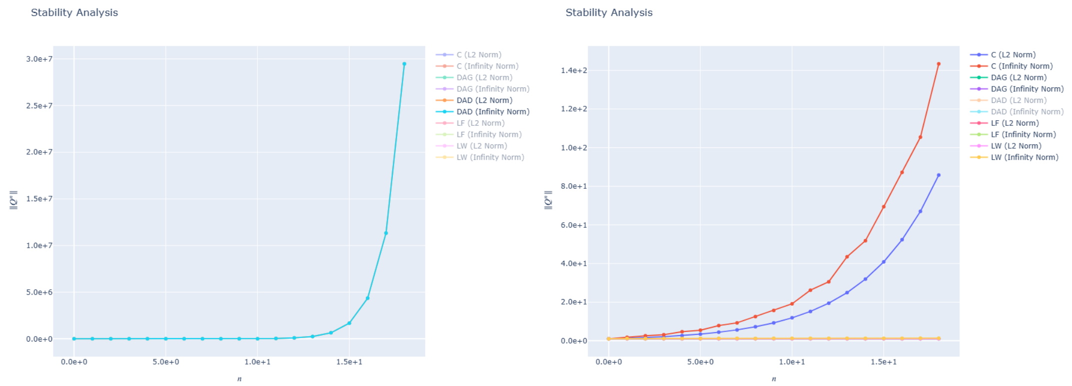

Figure 3.2: Numerical stability analysis

Indeed, we observe that $\|Q^n\|$ blows up in both the infinity norm and the 2-norm for the *décentré à droite* and *centré* schemes, while for the other schemes, the norm remains bounded by 1.

3.3 Convergence

Figure 3.3: Order of convergence

Since Δx and Δt are related through λ, we can restrict the convergence analysis to just Δx. Looking at the error of the unstable schemes, we observe that the error increases even as Δx becomes smaller. In contrast, for the stable schemes, the error aligns with Δx (order 1). This behavior is as expected for the *décentré à gauche* and Lax-Friedrichs schemes. However, for the Lax-Wendroff scheme, we would have expected an order of 2, meaning the error should align with Δx^2.

4 Conclusion

The transport equation with constant speed has been numerically solved. Five schemes have been implemented, of which three are not only consistent but also stable, and thus, by the Lax theorem, convergent. This has been confirmed both theoretically and in the results.

Order 1 convergence was the best achieved. The Lax-Wendroff scheme was promising with an expected order of 2 in theory, but it did not meet this expectation. It is possible that the theoretical convergence condition needs to be further adjusted to align with the practical implementation (as in TP 5) to achieve the theoretical result or even reach superconvergence.